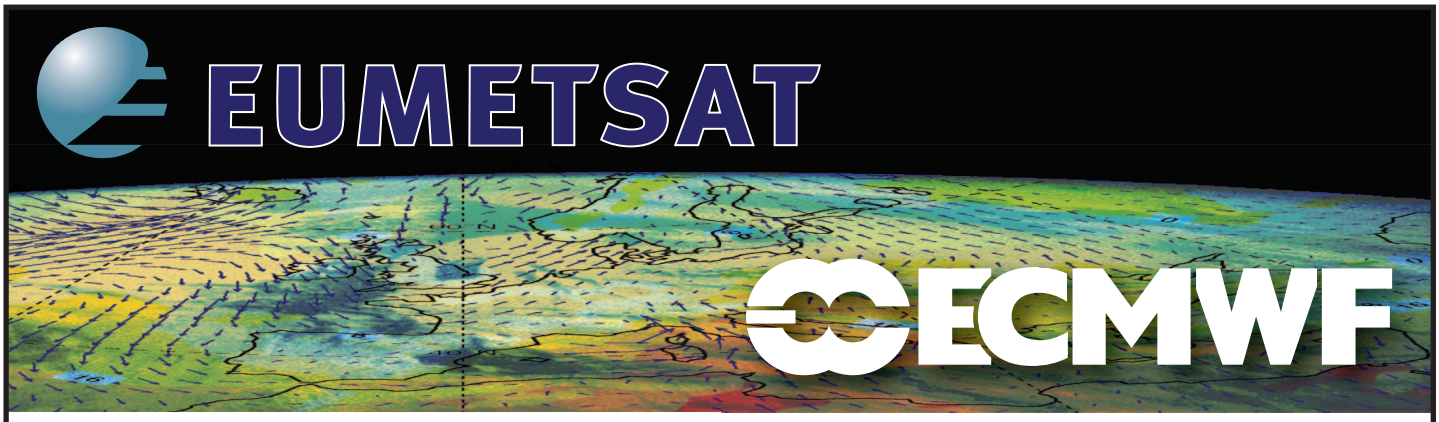

EUMETSAT/ECMWF Fellowship Programme
Research Report No. 26

Assimilation of ATOVS radiances at ECMWF: second year EUMETSAT fellowship report

E. Di Tomaso and N. Bormann

August 2012

Series: EUMETSAT/ECMWF Fellowship Programme Research Reports

A full list of ECMWF Publications can be found on our web site under:
http://www.ecmwf.int/publications/

Contact: library@ecmwf.int

©Copyright 2012

European Centre for Medium Range Weather Forecasts
Shinfield Park, Reading, RG2 9AX, England

Literary and scientific copyrights belong to ECMWF and are reserved in all countries. This publication is not to be reprinted or translated in whole or in part without the written permission of the Director-General. Appropriate non-commercial use will normally be granted under the condition that reference is made to ECMWF.

The information within this publication is given in good faith and considered to be true, but ECMWF accepts no liability for error, omission and for loss or damage arising from its use.

1 Executive summary

This report summarises work towards enhancing the usage of satellite observations from microwave sounders in the ECMWF system over surfaces which are particularly difficult to model, such as land, high orography and sea ice.

We have investigated the active assimilation over land of channel 5 radiances of the Microwave Humidity Sounder (MHS). Channel 5 is sensitive to low-level humidity as it is the lowest-peaking of the MHS channels in the 183 GHz water vapour band. Before this study, MHS channel 5 was assimilated at ECMWF only over sea, due to uncertainties in the estimated surface emission. The implementation of the dynamic retrieval of land surface emissivities has led to a better representation of model-estimated brightness temperatures over land compared to the previous static scheme, providing a good basis for the exploitation of additional surface-sensitive measurements.

Assimilation experiments during the AMMA period show that the active assimilation of channel 5 has a systematic impact on the mean moisture analysis, particularly over South America, Central and Western Africa and South/West Asia. The effect on the total column water vapour (TCWV) analysis has been validated in different years against independent GPS measurements from ground stations, and it is shown to be in most cases significant both in terms of correlation and mean TCWV over the experiment period. This is a noteworthy result provided by the assimilation of a single additional sounding channel. Furthermore, the assimilation of channel 5 over land improves the fit to other MHS observations already present in the system which provides an indication of an improved short-term forecast.

Results of assimilation experiments show that the use of MHS channel 5 over land has a neutral to positive impact on the forecast of temperature and humidity. As result of these studies, MHS channel 5 is actively assimilated over land at ECMWF since 19 June 2012 (CY38R1).

Additionally to the assimilation of an extra surface-sensitive channel, in the second part of the report a new screening criterion has been tested to screen out radiance observations with too large a contribution from the surface. The new criterion replaces the screening for high orography currently used for the Advanced Microwave Sounding Unit-A (AMSU-A) channel 5 and 6, and MHS channel 3 and 4, and it is used in our experiments also for MHS channel 5. Surface-sensitive observations are rejected over high orography because of a too large surface contribution to the observed radiation. In some cases, high orography is particularly difficult to model due to large inhomogeneity of the observed field of view. However the dynamic estimation of emissivities from observations makes this issue less severe. Furthermore, the current orography screening rejects the observations irrespectively of the instrument scan angle and does not take into account the fact that the ones at outer scan positions are less sensitive to the surface (as the atmospheric path increases away from nadir).

The new screening criterion is based on τ, the transmittance from the surface to space. A single threshold has been used globally for each of the 5 relevant AMSU-A and MHS surface-sensitive channels. These thresholds have been estimated from statistics of departures of observations from model estimates. The τ thresholds allow a more homogeneous coverage of the microwave sounding surface-sensitive channels with a considerable additional number of observations assimilated in particular at outer scan positions (as those observations are less sensitive to the surface than the ones near nadir).

Results of assimilation experiments suggest that a unique global threshold per channel might not work well to screen out observations which are difficult to model while including the ones that are useful to constrain the analysis. We suggest as alternative to the current screening of surface-sensitive observations from microwave

sounders, the use of an observation error which would take into account surface characteristics such as skin temperature and emissivity errors. Currently a unique value per channel is used globally to represent the observation error for AMSU-A and MHS.

In the last part of the report, we investigate an extension of the use of MHS data, namely over sea ice surfaces. MHS observations are currently assimilated operationally only over surfaces with skin temperature $TS \geq 278$ K and over low orography. The constraint on the skin temperature means that there is no humidity sounding coverage in most of the areas of the Globe with latitudes larger than ± 60 deg which include sea ice. As for the assimilation of microwave sounder data over land, the dynamic retrieval of emissivities provides a good basis for the use of MHS sounding also over sea ice.

We have tested three ways of retrieving the emissivities over sea ice for the simulation of the actively assimilated MHS measurements. This has allowed the assimilation of a considerable amount of humidity sounding observations in data sparse areas of the Globe. Retrieving emissivities at 157 GHz and using them (without any correction) for the water vapour channels has caused a clear improvement to the fit of MHS channel 3 and 4 observations both in the Northern and Southern Hemisphere. Furthermore, removing the current skin temperature constrain on the assimilation of MHS measurements over sea has allowed a great number of additional observations to be used over sea at high latitudes.

Results of assimilation experiments are encouraging towards a more extensive exploitation of MHS observations over sea and sea ice (they are extremely positive for the forecast of the temperature, geopotential and winds in the Southern Hemisphere), though they show that the additional data are introducing small biases which gradually corrupt slightly the first-guess in the Northern Hemisphere. In particular we have to reconsider relaxing the usage of MHS channel 5 measurements over sea as those observations in dry atmospheric conditions are considerably sensitive to the surface and not well modelled.

The structure of the report is as follows. First we present the results on the active assimilation over land of MHS channel 5, we then discuss the screening of microwave sounder surface-sensitive channels by transmittance, and subsequently we allow for the assimilation of water vapour observations over cold sea and sea ice. Final remarks follow at the end of the report.

2 Active assimilation of AMSU-B/MHS channel 5 over land

We have investigated the active assimilation over land of channel 5 radiances of the Microwave Humidity Sounder (MHS). This instrument is on-board three satellites, namely NOAA-18, NOAA-19 and MetOp-A. Channel 5 is sensitive to low-level humidity as it is the lowest-peaking of the MHS channels in the 183 GHz water vapour band. This channel is currently assimilated at ECMWF only over sea, due to uncertainties in the estimated surface emission. Emissivities for the simulation of microwave sounder radiances are calculated at ECMWF using a dynamic retrieval scheme, based on re-arranging the radiative transfer equation for window channel observations and using the ECMWF model background field (Karbou et al. 2005). The implementation of the dynamic retrieval of land surface emissivities has led to a better representation of model-estimated brightness temperatures over land (Bormann et al. 2009) compared to the previous static scheme, providing a good basis for the exploitation of additional surface-sensitive measurements, such as MHS channel 5.

The work in this section follows the one done by Fatima Karbou at Meteo-France (Karbou et al. 2010) where channel 5 is already actively assimilated over sea, low orography (less than 1000 m) and low latitudes (between ± 55 deg).

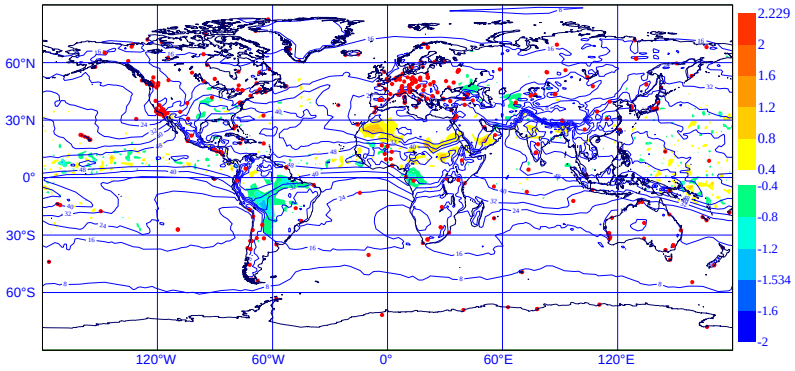

Figure 1: Mean TCWV analysis differences between the "channel 5 exp (2006)" and the "ctl exp(2006)" in kg/m^2. Contour lines represent mean TCWV analysis in the control experiment. The red dots indicate the locations of AMMA stations in Central Africa and IGS stations around the Globe.

2.1 Assimilation experiment setup

We have initially run assimilation experiments with active AMSU-B/MHS channel 5 observations over land in two summer periods from July to September in 2006 and 2010, using the ECMWF 4D-Var assimilation system at a T511 resolution. Emissivities for channel 5 over land are dynamically calculated from channel 1 (89 GHz). In order to test the assimilation of MHS channel 5 for an operational implementetion in the next ECMWF cycle upgrade (CY38R1), experiments were run in a second stage also in the winter (January to March) and summer (June to August) period of 2011 together with some fixes to the estimation of emissivities (see Appendix).

In the "channel 5 exp (2006)" channel 5 is assimilated over sea and low orography (less than 800 m), while in the "ctl exp (2006)" channel 5 is assimilated only over sea. Both experiments reject MHS observations where the skin temperature is lower than 278 k, and were run with the additional assimilation of MERIS data (which were not active in 2006 in the ECMWF system). Experiments were run in the 2006 period to be able to validate the results against GPS measurements from the African Monsoon Multidisciplinary Analysis (AMMA) campaign (Bock et al. 2008). Also GPS measurements from the IGS network (Dow 2009) were used for the validation of changes in the humidity field. The experiments run in the 2010 and 2011 periods, namely the "channel 5 exp (2010)" and "channel 5 exp (2011)", have the same settings for channel 5 as the 2006 experiments, but use a different observational system (for example they include the assimilation of MetOp-A and NOAA-19).

The results of the above experiments are given in the next section. They are quite consistent among the different experiments so, for convenience, we will focus on the aspects that can be found in all the experiments.

2.2 Results

2.2.1 Departure statistics

The assimilation of AMSU-B/MHS channel 5 over land has a relevant impact on the mean humidity analysis in all the experiments. Figure 1 shows the mean total column water vapour (TCWV) analysis differences between the "channel 5 exp (2006)" and the "ctl exp(2006)" averaged over a month. These differences are a few percent of the total TCWV value, and affect mainly the Tropical region.

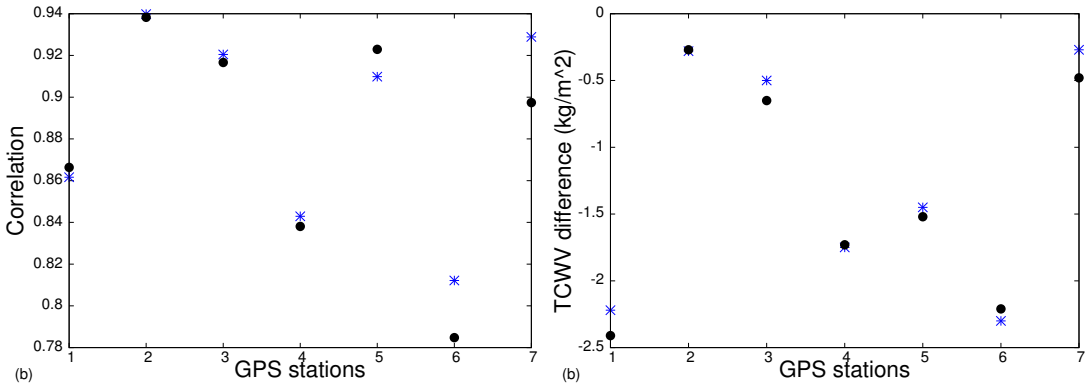

Figure 2: Correlation (a) and average differences (b) between the experiment analysis in the "channel 5 exp (2006)" (blue asterisks) and in the "ctl exp (2006)" (black circles) versus the GPS TCWV at six AMMA stations (Djougou (Benin), Niamey (Niger), Gao (Mali), Tamale (Ghana), Ouagadougou (Burkina Faso), Tombouctou (Mali)), and at the Gabon IGS station.

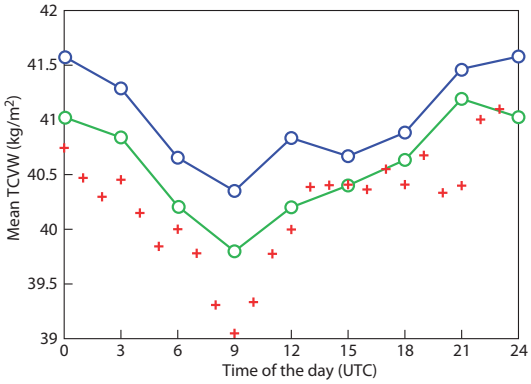

Figure 3: TCWV diurnal cycle at Gabon station for the "channel 5 exp (2006)" (green circles), the "ctl exp (2006)" (blue circles), and GPS measurements (red pluses).

Similar differences are also seen for the experiments run in the 2010 and 2011 period. We have investigated whether these changes agree with the information provided by the independent GPS observations available in 2006. Figure 2a shows the correlation over time between the experiment analysis ("channel 5 exp (2006)" (blue asterisks) and "ctl exp (2006)" (black circles)) and the GPS TCWV at seven GPS stations, while Figure 2b shows their average differences. The effect of MHS channel 5 on the TCWV is significant both in terms of correlation and mean TCWV at a few stations. We have identified an IGS station in Central Africa, in Gabon, where there is a relevant impact on the mean humidity analysis. We have estimated the TCWV diurnal cycle for the "channel 5 exp (2006)" and the "ctl exp (2006)" using analysis and short term forecast fields in the vicinity of the Gabon station (Figure 3). The shift in bias during the whole diurnal cycle in the "channel 5 exp (2006)" compared to the "ctl exp (2006)" indicates that the systematic drying over Central Africa is consistent with the GPS measurements in Gabon. The diurnal cycle appears to be well-represented with or without the assimilation of the additional channel, in contrast to (Karbou et al. 2010) who found a flat diurnal cycle for their control experiment.

The impact of MHS channel 5 on the humidity field has been validated also in the 2011 period using independent GPS observations from stations from the UCAR and Suominet network (Ware et al. 2000). Only a small number of stations are located in places where channel 5 has a relevant impact, and for some of them the

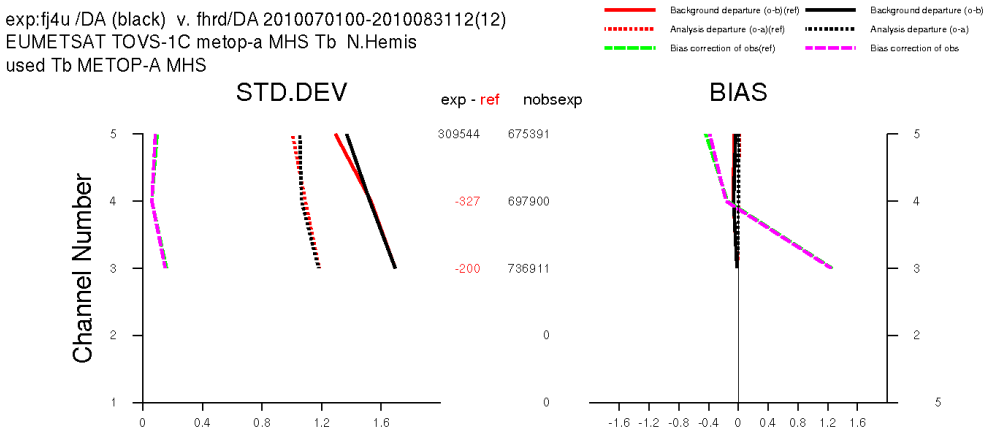

Figure 4: MetOp-A MHS brightness temperature departure statistics for the “channel 5 exp (2010)” (black) and the “ctl exp (2010)” (red) for the Northern Hemisphere.

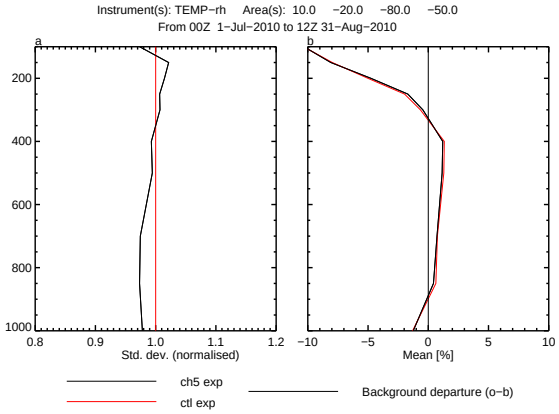

Figure 5: Radiosonde humidity departure statistics for the “channel 5 exp (2010)” (black) and the “ctl exp (2010)” (red) for an area of South America. The standard deviations have been normalised to the control experiments.

validation of “channel 5 exp (2011)” is again positive.

Departure statistics for the assimilated observing system were computed over the three month periods after the bias correction of satellite radiances. We show here for convenience only the results related to the 2010 or 2011 experiments, as there were no relevant differences between the different periods. The standard deviation of the differences between MHS channel 4 observations and model background (a short term forecast) for the “channel 5 exp (2010)” (black) and the “ctl exp (2010)” (red) are in Figure 4. The small increase in the standard deviation for channel 5 in the “channel 5 exp (2010)” is due to the additional data over land for which the estimate for the surface emission is still poorer than that over sea. The assimilation of channel 5 improves the fit to MHS channel 4 observations (there is a small improvement in the standard deviation of channel 4 compared to the control experiment). Also the fit to radiosonde observations in an area of South America (where a relevant impact is observed in the analysis) is slightly improved in the lower levels: Figure 5 shows the mean and standard deviation of radiosonde humidity observation departures from model estimates in the “channel 5 exp (2010)” (black) and in the “ctl exp (2010)” (red).

Figure 6 shows the fit to TCWV observed by the MERIS sensor on board of the Envisat satellite averaged over

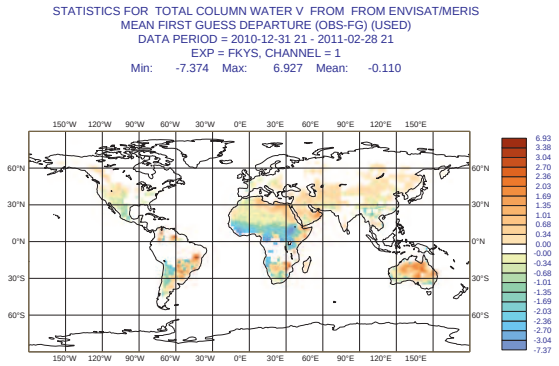

Figure 6: MERIS TCWV first-guess departures (in kg/m^2) for the "channel 5 exp (2011)" over January and February 2011.

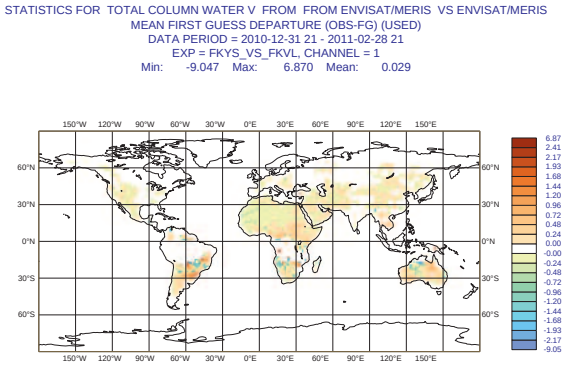

Figure 7: Difference of MERIS TCWV first-guess departures (in kg/m^2) between the "channel 5 exp (2011)" and the "ctl exp (2011)" over January and February 2011.

2 months of 2011 in the "channel 5 exp (2011)". A similar bias is observed for MERIS TCWV when MHS channel 5 is not active over land. The difference of the bias between the "channel 5 exp (2011)" and the "ctl exp (2011)" shows however that the assimilation of MHS channel 5 reduces partially the wet bias in Central Africa (Figure 7) as the "channel 5 exp (2011)" first-guess of TCWV in this region is drier than the "ctl exp (2011)" first-guess. A greater number of MERIS observations are assimilated in the same area of Central Africa when MHS channel 5 is active over land (Figure 8). The latter result suggests a better quality of the first-guess over this area.

2.2.2 Forecast impact

The experiment impact on the forecast has been studied for different variables and forecast ranges and results were computed for 3 months of assimilation experiments. The forecast impact is neutral in most cases when channel 5 is assimilated over land, which is consistent with a relatively small impact of these observations on the analysis. Forecast scores are shown in Figure 9 for forecast of the geopotential in the "channel 5 exp (2011)" in the winter period which includes also the fixes to the estimation of emissivities described in the Appendix.

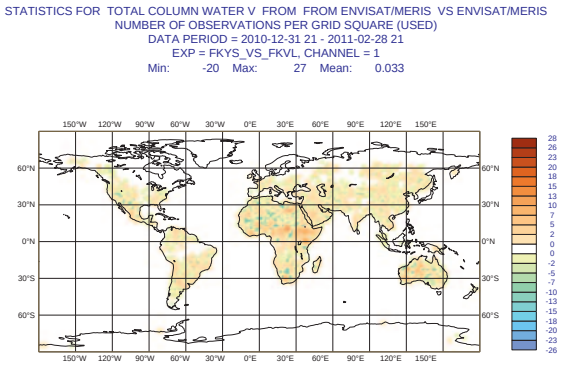

Figure 8: Counts differences for MERIS TCWV observations between the "channel 5 exp (2011)" and the "ctl exp (2011)" over January and February 2011.

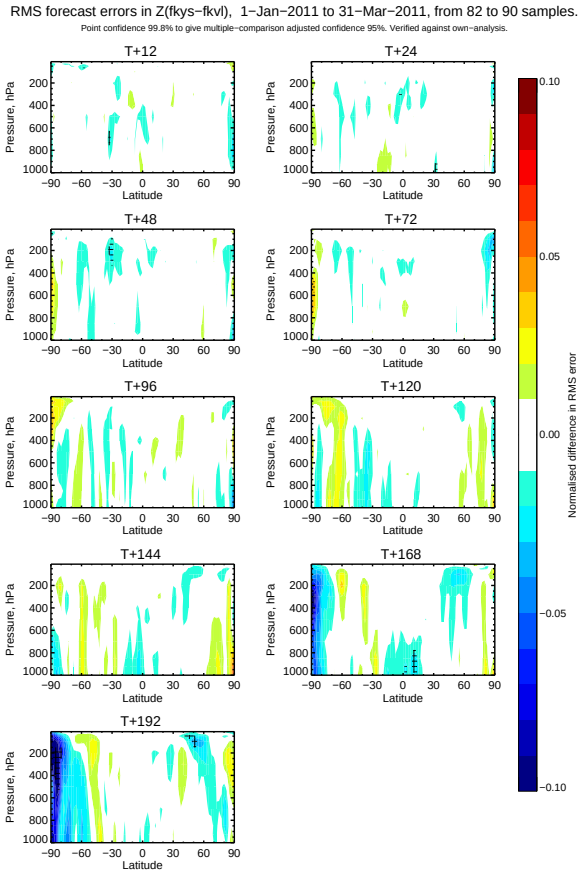

Figure 9: Normalised differences in the root mean square forecast error between the "channel 5 exp (2011)" (fkys) and the control experiment (fkvl) for the 0Z forecast of geopotential at different pressure levels. Verification is against the experiment own-analysis.

2.3 Conclusions

The active assimilation of MHS channel 5 over land provides low-level humidity information which has been positively evaluated against independent GPS measurements. Furthermore it improves the fit to other observations already in the system: in particular there is evidence of a better first-guess for MHS channel 4 (a channel also in the water vapour band, peaking above channel 5). The emissivities used for the simulation of MHS radiances are dynamically retrieved from MHS channel 1 (89 GHz) and the ECMWF background field. As result of these studies, MHS channel 5 is now actively assimilated over land in the latest ECMWF operational cycle (CY38R1).

3 Transmittance screening

Observations with a relevant contribution from the surface are not currently assimilated in the ECMWF operational analysis system due to large uncertainties in modelling accurately the surface emission. Window channels, i.e. channels where the atmospheric contribution to the observed radiation is relatively small compared to the surface contribution, are not assimilated in any part of the globe. Some of them are however used for quality control purposes (e.g. cloud/rain screening) and for calculation of surface emissivities. This is the case for AMSU-A channel 3 and 4 and MHS channel 1 and 2.

Observations with a minor, but not negligible, surface contribution are subject to an a priori screening over certain areas of the Earth: in particular tropospheric level data are not used over high orography. Figure 10 shows the coverage for MHS channel 3 and 4, and AMSU-A channel 5 and 6 observations operationally used to produce the atmospheric analysis. A number of fixed thresholds (see Table 1) are used at ECMWF to reject a priori data from these channels over high orography. In the rest of the section we will refer to this stage of the quality control as orography screening. Surface-sensitive observations are rejected over high orography because of a too large surface contribution to the observed radiation. In some cases, high orography is particularly difficult to model due to large inhomogeneity of the observed field of view: it is more difficult to specify accurately the mean characteristics of the observed surface. However the dynamic estimation of emissivities from observations (as it is currently done at ECMWF for AMSU-A and MHS) considers the inhomogeneity of the field of view making this issue less severe.

The current orography screening rejects the observations irrespectively of the instrument scan angle and does not take into account the fact that the ones at outer scan positions are less sensitive to the surface (as the atmospheric path increases away from nadir). The channel transmittance from surface to space (namely τ) indicates how sensitive the channel is to the surface and hence it can be exploited to screen observations that are too sensitive.

Table 1: Thresholds on the orography for the screening of AMSU-A and MHS surface-sensitive channels

Sensor	Channel	Latitude	Orography Threshold [m]
AMSU-A	channel 5	extra-Tropics	500
		Tropics	1000
	channel 6	extra-Tropics	1500
		Tropics	2000
MHS	channel 3	global	1500
	channel 4	global	1000

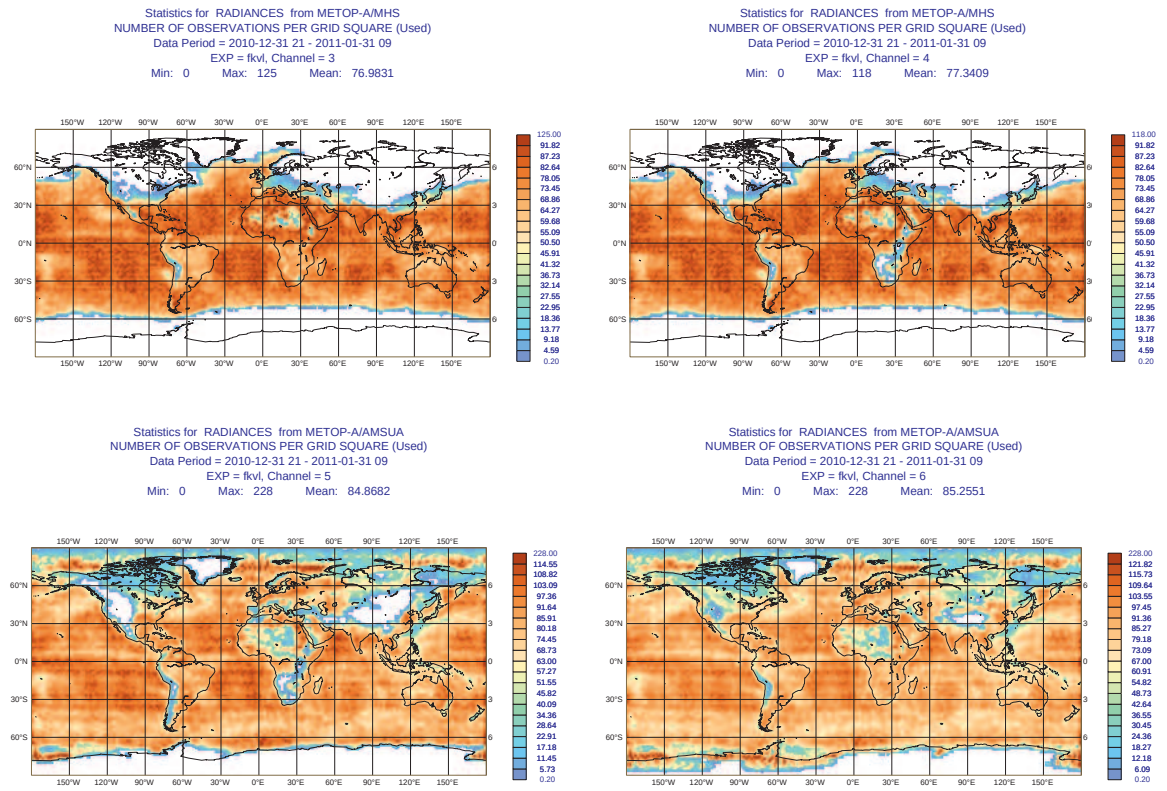

Figure 10: Number of MHS channel 3 (top left), channel 4 (top right), and AMSU-A channel 5 (bottom left) and channel 6 (bottom right) observations per grid box used in the atmospheric analysis in the control experiment (and similarly operationally) in January 2011.

Here we review the orography screening including also the assimilation of MHS channel 5 over land. In the rest of this section we will refer to AMSU-A channel 5-6 and MHS channel 3-5 as surface-sensitive channels. Their transmittance from surface to space varies from channel to channel: for example for AMSU-A channel 5 and 6 is respectively 0.12 and 0.02, as calculated by Alan Geer (ECMWF) for a representative sample of atmospheric profiles over sea and for close to nadir viewing angles. The transmittance value for MHS sounding channels varies greatly according to the humidity field.

3.1 Estimation of the screening thresholds

We have used the statistics of observation departures from model estimates to identify a suitable threshold to screen the surface-sensitive channels of AMSU-A and MHS. Figure 11a and 12a show binned standard deviations of first-guess departures for AMSU-A channel 5 and channel 6 for data over land not rejected by quality control (i.e. clear-sky data). Observations for all scan positions except the three outermost fields of view have been taken into account in the calculations. Figure 11b shows AMSU-A channel 5 counts used for the binned calculations in Figure 11a. It can be noted that most channel 5 observations have a transmittance value around 0.14.

The figures below show the expected behaviour: standard deviations of first-guess departures increase with increasing sensitivity to the surface (increasing τ) as errors in the modelling of the surface emission become

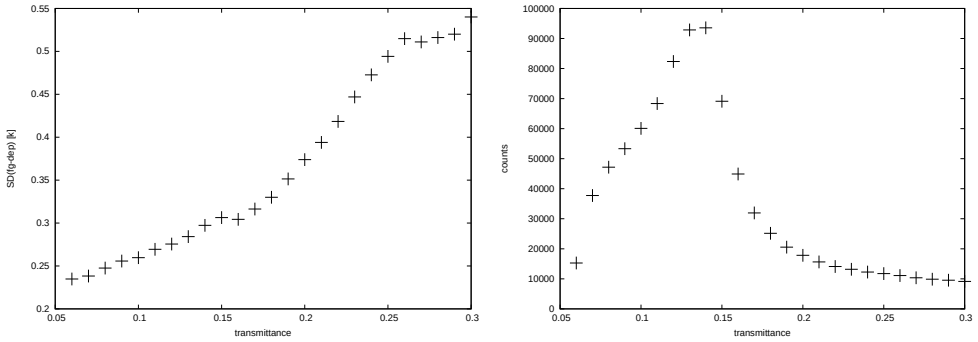

Figure 11: (a) Mean values of standard deviations of first-guess departures for AMSU-A channel 5 in a 0.01 transmittance bin for clear-sky data over land. (b) AMSU-A channel 5 counts used in the calculations of part (a) of this figure.

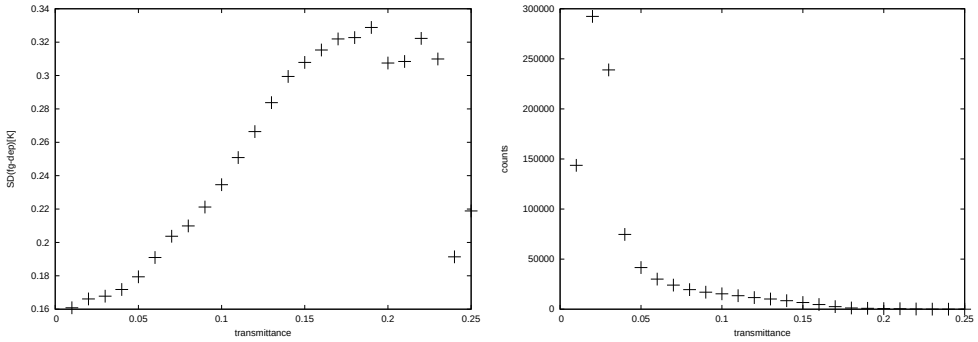

Figure 12: Same as for Figure 11 but for AMSU-A channel 6.

more relevant (English 2008). A threshold for τ of 0.15 for channel 5 corresponds to the exclusion of observations with standard deviations of first-guess departures greater than 0.3 K. This is consistent with the fact that at ECMWF the observation error for channel 5 is currently set to 0.28 K. For AMSU-A channel 6, the 0.06 threshold ensures that standard deviations of first-guess departures stay, on average, below around 0.2, the value currently used as a (fixed) observation error for channel 6. Note that we neglect here variations by surface type, and instead choose global thresholds.

3.2 Assimilation experiment setup

We have run a set of experiments testing different screening of AMSU-A and MHS surface-sensitive channels. In the rest of the section we call control experiment the experiment using orography thresholds and τ experiments the one using transmittance thresholds.

Here we show the results of two experiments using a 0.06 threshold on the transmittance for AMSU-A channel 6 and a 0.15 threshold for all the other surface-sensitive channels (AMSU-A channel 5 and MHS channel 3-5). The experiments ran with cycle CY37R3 in two seasons: from January to February 2011 and from June to July 2011. For AMSU-A the τ screening has been applied over land only, while for MHS it has been applied everywhere. The screening of MHS data also over sea was not intentional and we will have to take this into account when examining the results of the experiments. The assimilation of MHS channel 5 over land and the fixes to the estimation of the emissivities, as explained in Section 2 and in the Appendix, are also included in these experiments as in the control experiments. The control experiments are identical to the τ experiments

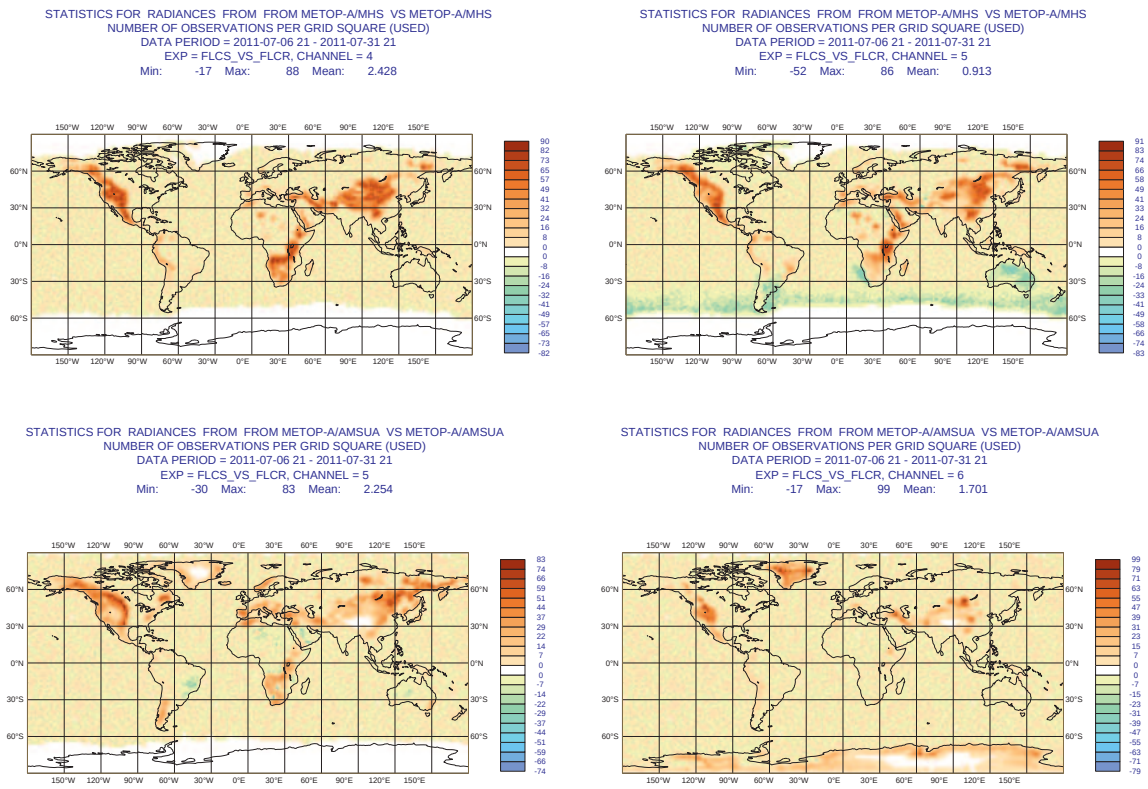

Figure 13: Count differences of MHS channel 4 (top left), channel 5 (top right), and AMSU-A channel 5 (bottom left) and channel 6 (bottom right) observations per grid box used in the atmospheric analysis in July 7-31 2011 between the τ experiment and the control experiment.

except for the usage of the thresholds in Table 1 for the screening of high orography (a threshold of 800 m is used globally for MHS channel 5).

3.3 Results

Figure 13 shows observation count differences between the τ and the control experiments in the summer period. A greater number of observations is on average globally assimilated for AMSU-A channel 5 and 6 and MHS channel 3 and 4. Observation counts per sensor scan position show that these additional observations are assimilated in a greater number at outer scan positions compared to central scan positions (see Figure 14), while standard deviation of first guess departures for outer fields of view remain comparable to their nadir counterparts. As said earlier, the current orography screening rejects the observations irrespectively of the instrument scan angle and does not take into account the fact that the ones at outer scan positions are less sensitive to the surface.

There are however regions of the Globe where a decrease in the number of observations occurs for the lowest peaking channels: for MHS channel 5 this is the case for Australia, Argentina and the sea at about -50 deg latitude in the summer season (when these regions are particularly dry and the channel's weighting function peaks lower in the atmosphere), while for AMSU-A channel 5 a relatively small decrease of assimilated observations occur in some areas over land in the Tropics. In the winter season there is a smaller number of MHS channel 5

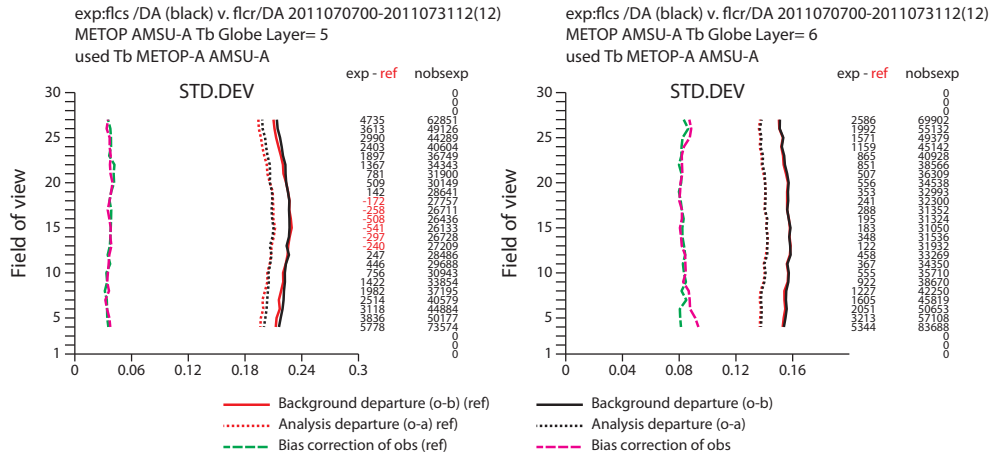

Figure 14: Mean standard deviation of first-guess departures for AMSU-A channel 5 (left) and channel 6 (right) on MetOp-A at different scan positions for the τ experiment (flcs) (black) and the control experiment (flcr) (red). Data counts are printed along the vertical axis on the right of the plot for the τ experiment (nobsexp) and for the difference between the τ experiment and the control experiment (exp-ref). The τ experiment uses a threshold 0.06 to screen channel 6 observations and a threshold 0.15 for the other surface-sensitive observations.

observations assimilated over the Northern Hemisphere over sea and over land, in particular over North Africa, compared to the control experiment. As explained earlier, the decrease of MHS channel 5 observations over sea was unintentional.

3.3.1 Departure statistics

A first way to assess the change in the data usage is to measure the impact of the new screening on the quality of the analysis and of the first guess studying the fit to conventional and satellite observations. Departure statistics (mean departures and standard deviations) for radiance observation types are computed after the bias correction of satellite radiances.

Departure statistics averaged over the Northern Hemisphere (extra Tropics), Tropics, and Southern Hemisphere (extra Tropics) show no significant change to the fit to radiosonde observations of temperature, winds and humidity, both in the summer and winter period (not shown). There is however a very small number of radiosonde observations that are not assimilated in the τ experiments compared to the control experiments which could imply a small degradation in the quality of the first-guess.

Maps of statistics of first-guess departures of observations from model estimates show that the τ threshold works quite efficiently in screening AMSU-A channel 5 observations over high orography but still allows a more homogeneous coverage than the orography threshold (Figure 15, left, shows the standard deviation of first departures for AMSU-A channel 5 observations, before bias correction, used in the atmospheric analysis). Statistics for AMSU-A channel 6 also show that in both seasons the standard deviations of first-guess departures in the regions where the τ screening has added a considerable number of observations are not higher than other parts of the Globe (Figure 16, right) . This is a very encouraging result towards enhancing the usage of AMSU-A surface-sensitive data at outer scan positions.

There are some differences in the mean first-guess departures for the AMSU-A channels: the biases for channel 6 are a bit larger (of about 0.5 k) over some of the regions of the new data, for example over Antarctica in the summer season (see Figure 16), and there are some differences in the AMSU-A channel 5 bias over Africa

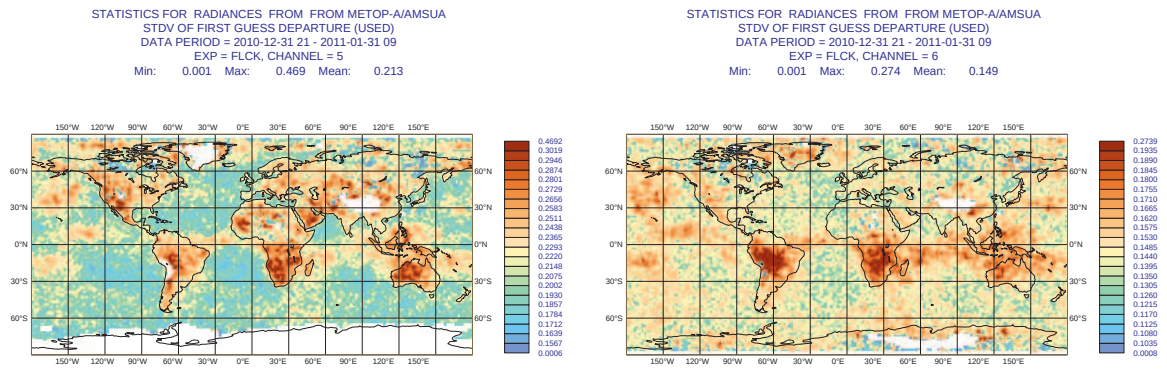

Figure 15: Global maps of mean standard deviations of first-guess departures for AMSU-A channel 5 (left) and channel 6 (right) on MetOp-A in January 2011 when a τ threshold 0.15 and 0.06 (respectively) is used to screen these observations.

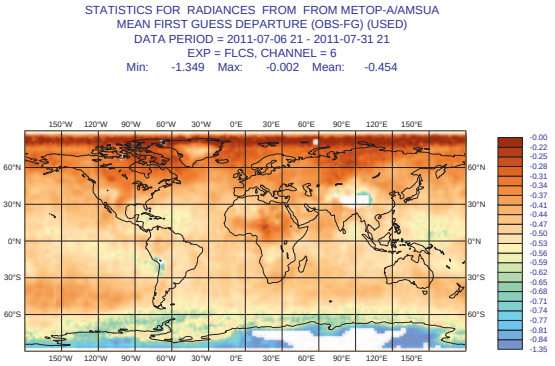

Figure 16: Global maps of mean first-guess departures, before bias correction, for AMSU-A channel 6 on MetOp-A in July 7-31 when a threshold 0.06 is used to screen the surface-sensitive observations.

compared to the control experiment, but these differences are quite small.

The standard deviations of first-guess departures averaged over the extra Tropics are larger in the τ experiments than in the control experiment for MHS channel 5, and to a lesser extent for channel 4, while there are no significant changes for channel 3. Global maps of first-guess departure statistics show that for channel 4 and 5 this is the case in the summer period when more observations with higher standard deviation (relatively to other areas of the Globe) are assimilated over land (for example around the Himalayan region), (see Figure 17). MHS observations in the same areas in the Northern Hemisphere are not assimilated in the winter season due to a screening based on the skin temperatures which aims to exclude snow-covered surfaces. Elsewhere and in the winter season the increase in the standard deviation of first-guess departures for channel 5 radiances is possibly due to fewer observations assimilated (unintentionally) over sea compared to the control (as sea observations tend to have lower standard deviations), particularly around -50 deg latitude in the summer and to a lesser extent in the winter experiment.

The differences in the analysis mean humidity field between the τ experiments and the control experiments are however relatively small (see Figure 18).

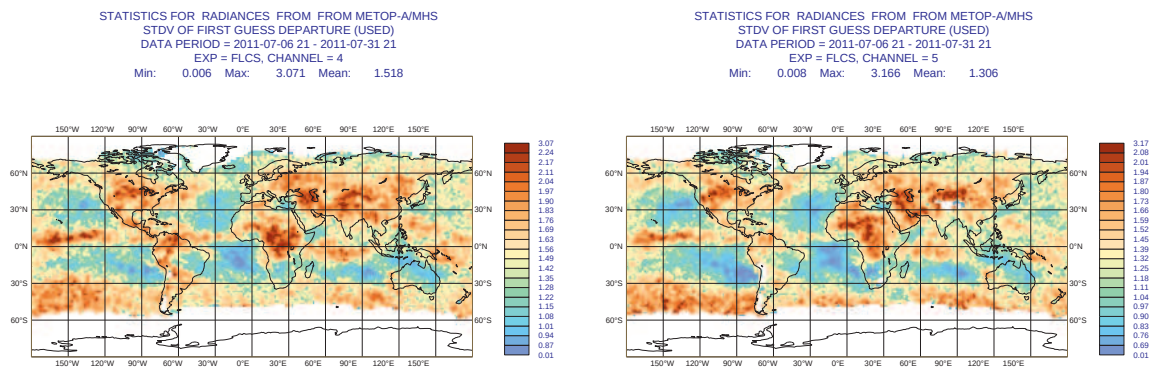

Figure 17: Global maps of mean standard deviations of first-guess departures for MHS channel 4 (left) and channel 5 (right) on MetOp-A in July 7-31 when a threshold 0.15 is used to screen the surface-sensitive observations.

3.3.2 Forecast impact

The experiments impact on the forecast is studied for different variables, regions and forecast ranges. Forecast results are computed for 61 days of assimilation experiments in both seasons.

In the summer period, for the forecast of the temperature the impact of the τ experiment versus the control experiment is negative in the Southern Hemisphere at about -50 deg latitude at low levels in the short-term, while it is neutral to positive elsewhere (see Figure 19). Overall the summer experiment performs better than the winter one. In the winter period the extent of the negative impact in the Southern Hemisphere is greater than in the summer period (see Figure 20): for example, it is significantly negative for the forecast of the temperature over the South Pole up to day 5 of the forecast.

Similar results are found for the forecast of the geopotential in both seasons.

We could speculate that the differences between the two seasons are consistent with a greater degradation of MHS channel 5 departures (due to fewer observations assimilated) in the winter season both in the Northern and Southern Hemisphere compared to the summer season. Global maps of forecast error differences seem to confirm that large negative scores originate from the ocean in the Southern Hemisphere but also from the Antarctic region (see for example Figure 21 for the forecast of the geopotential at 500 hPa). However, it is not straightforward to separate the impact of all the changes in data coverage contributing to the differences in forecast error between the τ experiments and the control experiments.

3.4 Conclusions

Thresholds on the transmittance τ from surface to space have been tested to screen out AMSU-A and MHS surface-sensitive observations with too large a contribution from the surface. These thresholds have been estimated from statistics of departures of observations from model estimates. A single threshold has been used globally for each of the 5 relevant AMSU-A and MHS surface-sensitive channels. The τ thresholds allow a more homogeneous coverage of the microwave sounding surface-sensitive channels with a considerable additional number of observations assimilated in particular at outer scan positions (as those observations are less sensitive to the surface than the ones near nadir).

Global averaged departures statistics for AMSU-A surface-sensitive channels did not increase with the addi-

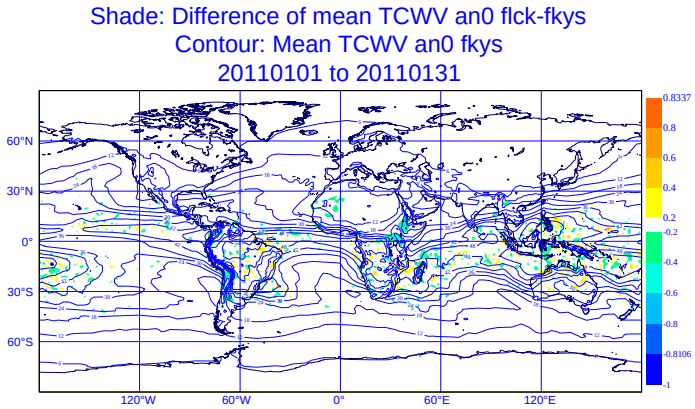

Figure 18: Mean TCWV analysis differences in kg/m^2 between the τ experiment and the control experiment in January 2011. Contour lines represent mean TCWV analysis in the control experiment.

tional observations. This is a very encouraging result towards an enhanced exploitation of AMSU-A channel 5 and 6 than what is currently done in operations. Departure statistics show some degradation to the fit of MHS surface-sensitive channels: this is due both to having relaxed too much their usage in dry atmospheric conditions (when these observations are considerably sensitive to the surface) and to the unintentional reduction of MHS observations over sea.

It would be interesting to explore this degradation further by testing the τ thresholds without the unintentional removal of data over sea. However, we find more opportune to pursue a different approach in order to enhance the usage of very important data such as the lower tropospheric observations of AMSU-A and the MHS water vapour observations. Results of assimilation experiments suggest that a unique global threshold per channel might not work well to screen out observations which are difficult to model while including the ones that are useful to constrain the analysis. A possible alternative to the current screening of surface-sensitive microwave sounder observations is to use an observation error which takes into account surface characteristics such as skin temperature and emissivity errors. This approach will down-weight data in areas where the error from the surface emissivity is larger, yet still allow such observations to influence the analysis, especially in data sparse regions.

4 Enhanced assimilation of microwave sounding data over sea and sea ice

MHS observations from channel 3, 4 and 5 (the 3 channels in the 183 GHz water vapour band) are currently assimilated operationally only over surfaces with skin temperature $TS \geq 278$ K and over low orography. The constraint on the skin temperature means that there is no humidity sounding coverage in most of the areas of the Globe with latitudes larger than ± 60 deg which include sea ice. The other two MHS channels (namely window channels) are used for emissivity retrieval over land (channel 1 at 89 GHz) and quality control purposes (channel 2 at 157 GHz).

As for the assimilation of microwave sounder data over land, the dynamic retrieval of emissivities provides a good basis for the use of MHS sounding over sea ice, as shown also in (Bouchard et al. 2010). The dynamic

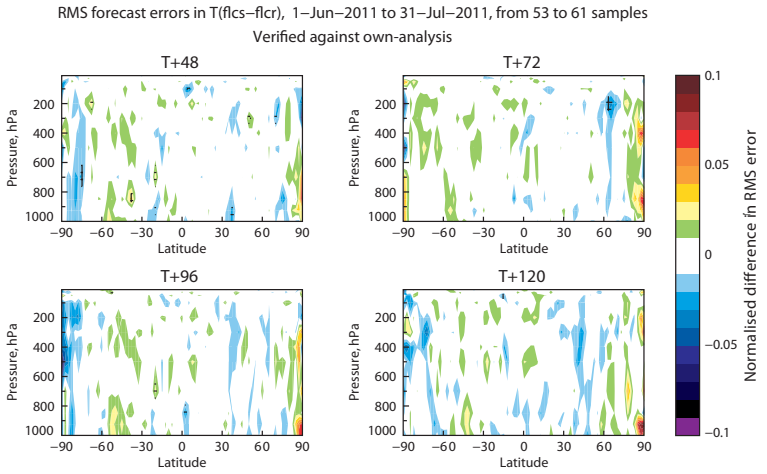

Figure 19: Normalised differences in the root mean square forecast error between the τ experiment (flcs) and the control experiment (flcr) for the 0Z forecast of the temperature at different pressure levels in the summer period. Verification is against the experiment own-analysis.

retrieval of emissivities is based on the assumption that the error introduced by using for a given frequency emissivities calculated at a different frequency is small. As shown earlier in this report, this is the case for MHS observations over land: departure statistics show that emissivities retrieved at 89 GHz can be used for the water vapour channels without introducing a subsequent bias. Over sea ice the situation is more complex as the emissivity spectra vary greatly with the type of ice (Harlow 2011). There are surfaces for which the emission at 89 GHz might be quite different than the one at 157 GHz or 183 GHz. These issues have been taken into account in the experiments described in the next section.

4.1 Assimilation experiment setup

We have run assimilation experiments with the active usage of additional MHS observations over sea and sea ice. Experiments were run at a low resolution (T319) with cycle CY37R3 from June to September 2011 with MHS channel 3, 4 and 5 active over sea with any skin temperature, and channel 3 and 4 active also over sea ice. The current constraint on the skin temperature has been left unchanged over land (i.e. MHS observations are assimilated only over surfaces with skin temperature $TS \geq 278$ K to exclude snow-covered surfaces). The assimilation of MHS channel 5 over land, the fixes in the estimation of emissivities (as described in the Appendix) and a fix to surface skin temperature (included to cycle CY38R1 by Ben Ruston) are also included in these experiments as in the control experiment.

The emissivities used in the simulation of radiances over sea ice are dynamically retrieved emissivities. We have considered two cases: the use of emissivities retrieved from channel 2 observations (at 157 GHz) (experiment EXP1) and the use of emissivities retrieved from channel 1 observations (at 89 GHz) (experiment EXP2). In both experiments the additional data over sea with $TS < 278$ K are simulated with FASTEM emissivities (Liu at al. 2011) (as it is done for all the other MHS observations over sea). These two experiments are identical to the control experiment (fnrk) except for the usage of observations over cold sea and sea ice.

The emissivities at 89 GHz might differ considerably from the ones at 183 GHz over certain surfaces. These differences are in general smaller for emissivities retrieved at 157 GHz. Therefore emissivities retrieved over sea ice at 89 GHz need to be corrected before being used to simulate the water vapour channels. In experiment

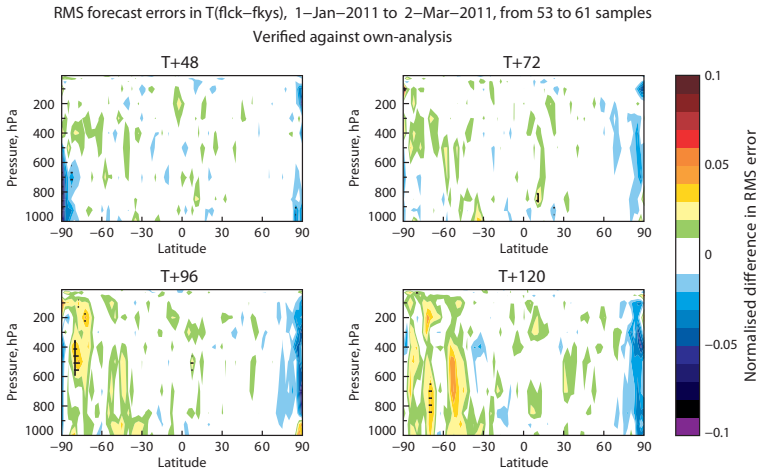

Figure 20: Normalised differences in the root mean square forecast error between the τ experiment (flck) and the control experiment (fkys) for the 0Z forecast of the temperature at different pressure levels in the winter period. Verification is against the experiment own-analysis.

EXP2, we have applied as correction term the one currently used in the Meteo France system based on the brightness temperature difference between channel 2 (TB_2) and 1 (TB_1), (Bouchard et al. 2010), as follows:

$$\begin{aligned} \varepsilon_{corrected} &= \varepsilon_{retrieved} + (TB_2 - TB_1)/TS - 0.01 \quad \text{if} \quad (TB_2 - TB_1)/TS > 0 \\ \varepsilon_{corrected} &= \varepsilon_{retrieved} + (TB_2 - TB_1)/TS - 0.02 \quad \text{if} \quad (TB_2 - TB_1)/TS \leq 0 \end{aligned} \tag{1}$$

The emissivities retrieved at 157 GHz are used in experiment EXP1 without correction for the water vapour channels, and with a correction (derived from the one above) for the 89 GHz channel (used in this experiment for quality control). Channel 2 is currently used at ECMWF as a quality control channel to screen out cloudy and rainy radiances: large absolute departures of channel 2 observations from model estimates are interpreted as a sign of cloud or rain affected radiances. We therefore have used channel 1 as a quality control channel in the experiment (EXP1) in which channel 2 is used for emissivity retrieval.

Table 2 summarises the settings used for the assimilation experiments described above plus an experiment (the last one in the table) which uses over sea ice emissivities calculated with an old scheme, known as the Kelly & Bauer scheme (Kelly and Bauer 2000). This static scheme is based on a classification of the surface type and an appropriate parametric model per surface type.

In all the experiments sea ice is identified as a surface having land-sea mask less than 0.1 and surface temper-

Table 2: Settings for the assimilation experiments on the enhanced use of MHS over sea and sea ice

Experiment name	Experiment ID	Emissivity estimation over sea ice	Emissivity correction over sea ice	Channel used for quality control over sea ice
EXP1	fnta	Retrieved from Channel 2	correction for Channel 1	Channel 1
EXP2	fnv8	Retrieved from Channel 1	correction for Channel 2-5	Channel 2
EXP3	fmqy	Kelly & Bauer scheme	NA	Channel 2

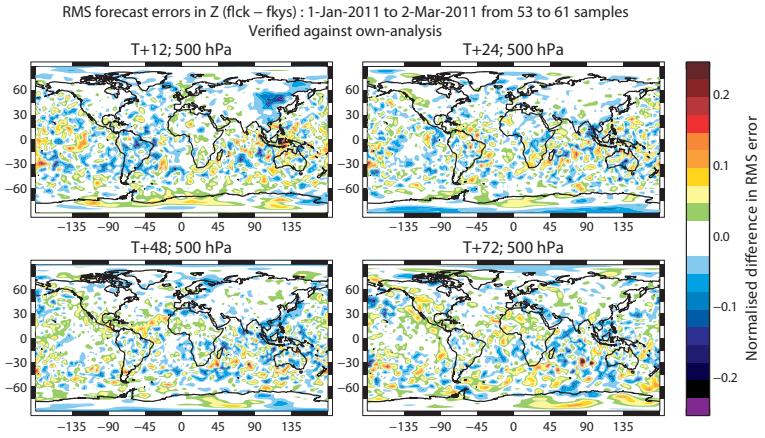

Figure 21: Global maps of normalised differences in the root mean square forecast error between the τ experiment (flck) and the control experiment (fkys) for the 0Z forecast of the geopotential at 500 hPa in the winter period. Verification is against the experiment own-analysis.

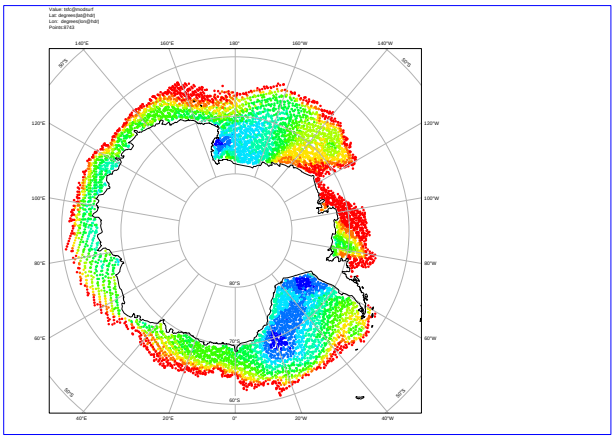

Figure 22: Sea ice extention over the South Pole on June 6 2011 estimated with land-sea mask less than 0.1 and surface temperature $TS < 271.45$ K. The colour scale indicated a TS from 242 K (blue) to 272 K (red).

ature $TS < 271.45$ K. Figure 22 shows the sea ice extention calculated with these two thresholds on one of the day in which the experiments ran.

4.2 Results

Figure 23 shows the difference in counts between the observations actively assimilated in experiment EXP1 and the control for MHS channel 4 and 5 (the plot for channel 3 is quite similar to the one for channel 4). A considerable number of additional MHS observations is assimilated in particular below -50 deg latitude, where there is no humidity sounding coverage in the control experiment (and similarly in the operational configuration).

A greater number of MHS channel 3 and channel 4 data are assimilated over sea ice in EXP1 compared to EXP2. This suggests that the emissivities calculated from 157 GHz, and used without a correction, might be more accurate than the ones calculated from 89 GHz, after a correction is applied to them. We need however to

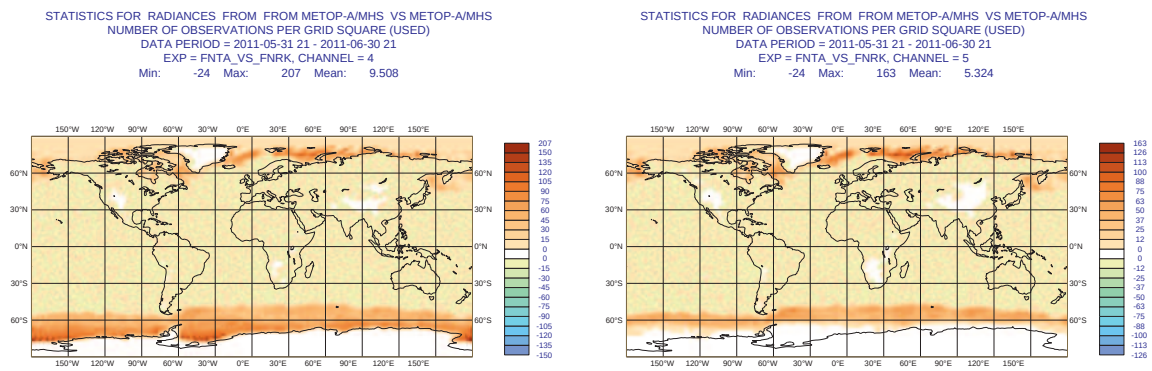

Figure 23: Count differences for MHS channel 4 (left), channel 5 (right) observations per grid box used in the atmospheric analysis between experiment EXP1 and the control experiment in June 2011.

take into account that a different quality control is used in the two experiments.

Most observations over sea ice are rejected in EXP3 due to very high departures between the observations and the first-guess, proving that the dynamic emissivities over sea ice are more accurate than the static ones calculated by the old Kelly & Bauer scheme. For this reason, we have run this experiment only for a short period, and we will not show below departure statistics and score results for experiment EXP3 as they will not be significant.

4.2.1 Departure statistics

As for the assimilation of microwave sounder data over land, using the dynamically retrieved emissivities over sea ice provides a better representation of model-estimated brightness temperatures than a static scheme. Figure 24 shows histograms of first-guess departures for MHS channel 3 (left), channel 4 (centre) and channel 5 (right) observations over sea ice when emissivities are estimated by the old Kelly & Bauer scheme (CTL, red), are retrieved dynamically from observations at 157 GHz (EXP1, green) or from observations at 89 GHz and with a correction for the variation of emissivities with frequency (EXP2, blue). Here all data have been considered, i.e. before any screening and quality control stage and before bias correction. Therefore, in the control experiment, emissivities over sea ice are estimated by the Kelly & Bauer scheme, though are not actively assimilated. The dynamic emissivities lead to improved simulations for the 183 GHz sounding channels (histograms for EXP1 and EXP2 are narrower and more centred around 0 than for the control experiment), and using the 157 GHz channel for the emissivity retrieval appears to perform best (the histogram for EXP1 is slightly narrower than for EXP2).

Global maps of mean differences between assimilated MHS measurements and observations simulated from the short-term forecast in experiment EXP1 show that the biases are large before bias correction for channel 4 over sea ice and channel 5 over cold sea in the Southern Hemisphere. These biases are reduced after bias correction, with the exception of channel 4 over sea ice (see Figure 25 for the bias of MHS channel 4 and channel 5 after bias correction), and are however not larger over sea ice and cold sea than other parts of the Globe.

The average standard deviation of first-guess departures for MHS channel 5 over the Southern Hemisphere is larger in the EXP1 than in the control experiment (see Figure 26). As shown with the transmittance studies in the previous section, MHS channel 5 peaks quite low in the atmosphere in the winter Hemisphere. We are therefore adding observations over sea in the Southern Hemisphere that are considerably sensitive to the surface

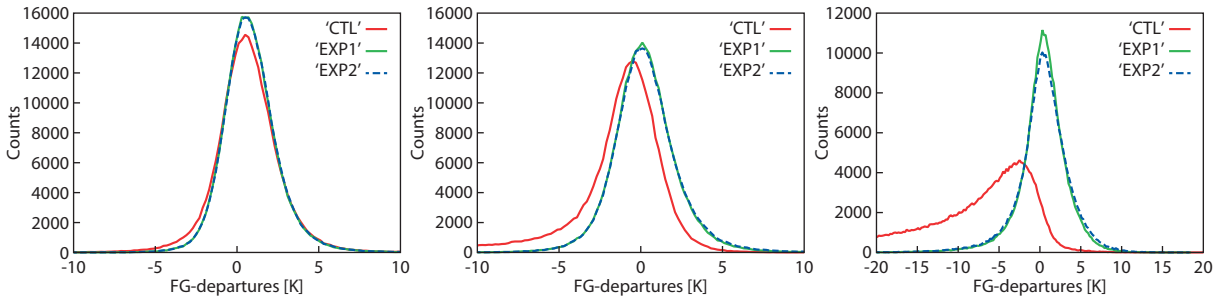

Figure 24: Histograms of first-guess departures for MHS channel 3 (left), channel 4 (centre) and channel 5 (right) over sea ice in July 2011 when emissivities are estimated by an old static scheme (known as the Kelly & Bauer scheme, CTL, red), are retrieved dynamically from observations at 157GHz (EXP1, green) or from observations at 89 GHz and with a correction for the variation of emissivities with frequency (EXP2, blue).

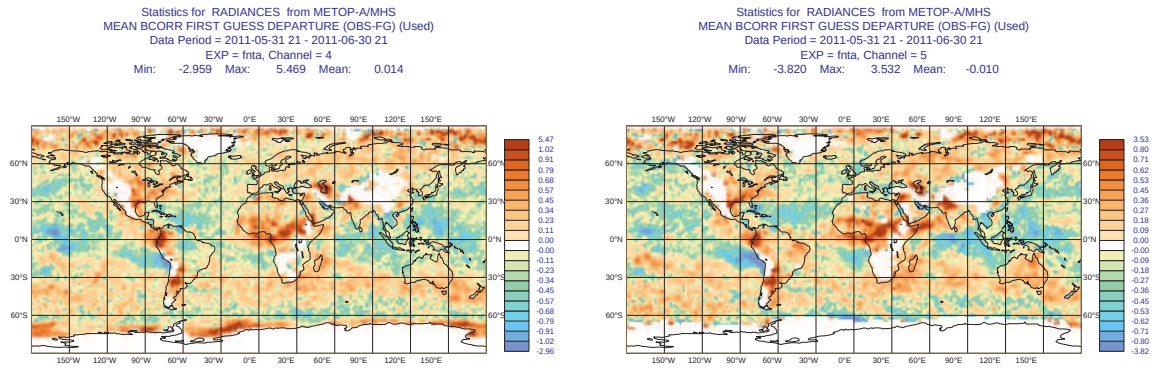

Figure 25: Global maps of mean first-guess departures after bias correction for MHS channel 4 (left) and channel 5 (right) on MetOp-A in experiment EXP1 (fnta) in June 2011.

and are not well modelled. The decrease in the standard deviation for MHS channel 3 and 4 observations in experiment EXP1 both over the Northern Hemisphere and the Southern Hemisphere and for channel 5 in the Northern Hemisphere is possibly due to the numerous additional data assimilated over sea (as sea observations tend to have lower standard deviations than land observations).

Departure statistics for experiment EXP2 are quite similar to the ones for experiment EXP1. However, bias and standard deviation of first-guess departures for assimilated MHS channel 4 measurements over the Southern Hemisphere are slightly smaller (and a greater number of observations is assimilated) in experiment EXP1 than in experiment EXP2 (see Figure 27). Global maps of first-guess departure statistics show that this is the case particularly over sea ice (see Figure 28). This is a further evidence of the better quality of the emissivities over sea ice in experiment EXP1 than in experiment EXP2.

4.2.2 Forecast impact

Forecast results are computed for different variables and regions for 92 days of assimilation experiments. The results in the Southern Hemisphere for EXP1 are very positive for the forecast of the temperature, geopotential and winds. The positive impact for forecast of the temperature appears statistically significant at 95% con-

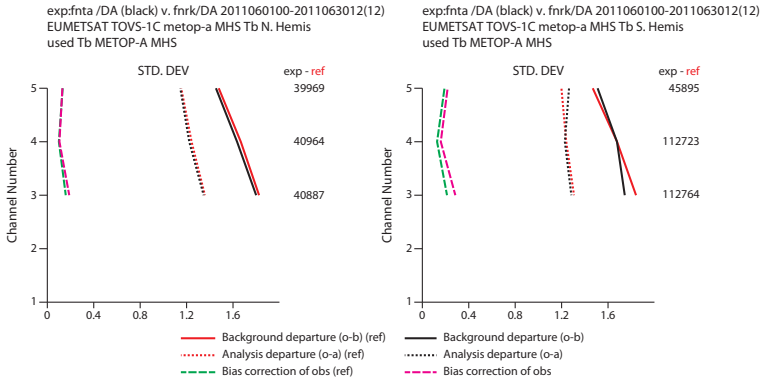

Figure 26: MetOp-A MHS brightness temperature departure statistics (standard deviations of first-guess departures) for the experiment EXP1 (fnta) (black) and the control experiment (fnrk) (red) for the Northern Hemisphere (left) and the Southern Hemisphere (right).

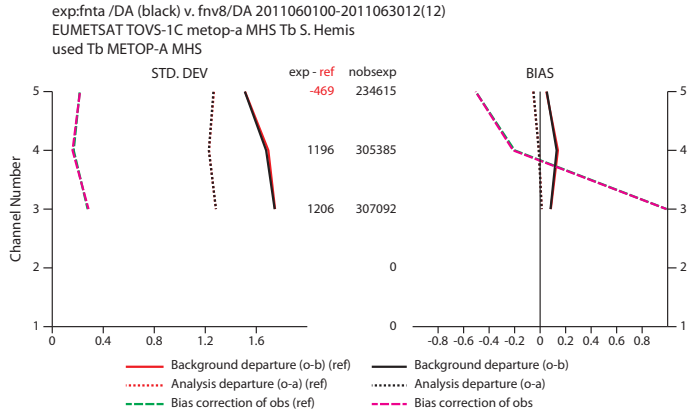

Figure 27: MetOp-A MHS brightness temperature departure statistics (standard deviations of mean first-guess departures (left) and mean first-guess departures (right)) for the experiment EXP1 (fnta) (black) and the experiment EXP2 (fnv8) (red) for the Southern Hemisphere.

fidence level for all the forecast days at 1000 hPa and from day 2 to 6 at 850 hPa, when averaged over the Southern Hemisphere (see Figure 29). There is however a neutral to negative impact in the Northern Hemisphere (see for example Figure 30 for the forecast of the temperature at different latitudes and pressure levels), which seems to be statistically significant at day 3 and 4 of the forecast.

Also experiment EXP2 shows a positive impact in the Southern Hemisphere for the forecast of all the relevant variables but the extent of the statistically significant negative impact in the Northern Hemisphere is greater in experiment EXP2 than in experiment EXP1. A test experiment in which the new data were added only in the Southern Hemisphere has shown the same pattern of the error (positive scores in the Southern Hemisphere and slightly negative scores from day 3 in the Northern Hemisphere). This suggests that the bias of the additional data in EXP2 (and to a lesser extent in EXP1) in the Southern Hemisphere causes, through the variational bias correction scheme (VarBC) (Dee 2004), a propagation of the error in the Northern Hemisphere few days into the forecast. The predictor coefficients for a linear bias model are in fact estimated globally within the VarBC framework.

Forecast scores show a considerable negative impact for relative humidity in the short range at the location of

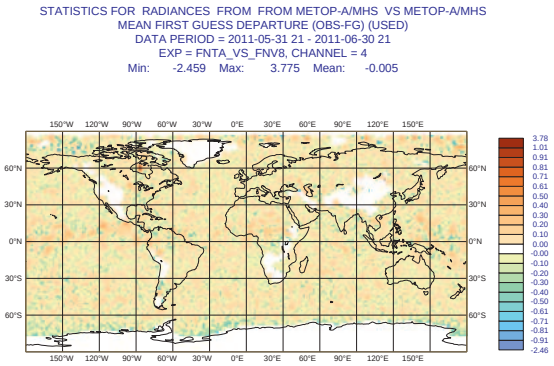

Figure 28: Global difference of mean first-guess departures for MHS channel 4 on MetOp-A between experiment EXP1 (fnta) and experiment EXP2 (fnv8) in June 2011.

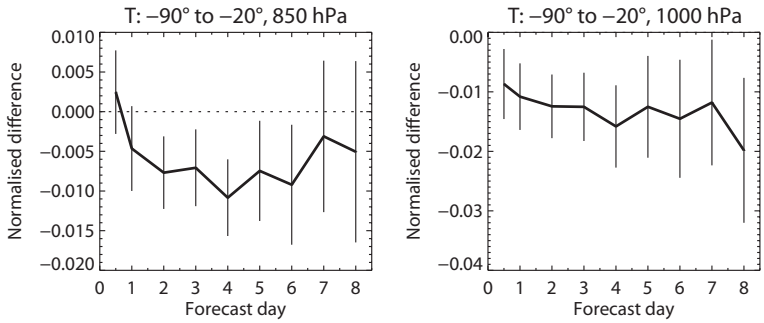

Figure 29: Normalised differences in the root mean squared forecast error between the experiment EXP1 (fnta) and the control experiment (fnrk) for the 0Z forecast of the 850 hPa and 1000 hPa temperature. Verification is against the experiment own-analysis.

the additional data assimilated in both experiment EXP1 and experiment EXP2 (see Figure 31). As argued in (Geer et al. 2009), this is likely an apparent degradation in the forecast error of the relative humidity due to adding humidity observations in a data-poor area and verifying using the experiment own-analysis as proxy of the true state of the atmosphere. The degradation is in fact not observed for the other atmospheric parameters, or in verification of short-term forecasts against observations.

4.3 Conclusions

The use of dynamically retrieved emissivities over sea ice has allowed the assimilation of a considerable amount of humidity sounding observations in data sparse areas of the Globe. Furthermore, removing the current skin temperature constrain on the assimilation of MHS measurements over sea has allowed a great number of additional observations to be used at high latitudes.

We have tested three ways of retrieving the emissivities over sea ice for the simulation of the actively assimilated MHS measurements. Retrieving emissivities at 157 GHz and using them (without any correction) for the water vapour channels allows the assimilation of MHS high peaking channels over sea ice with a clear improvement to the fit of MHS channel 3 and 4 observations both in the Northern and Southern Hemisphere. We have

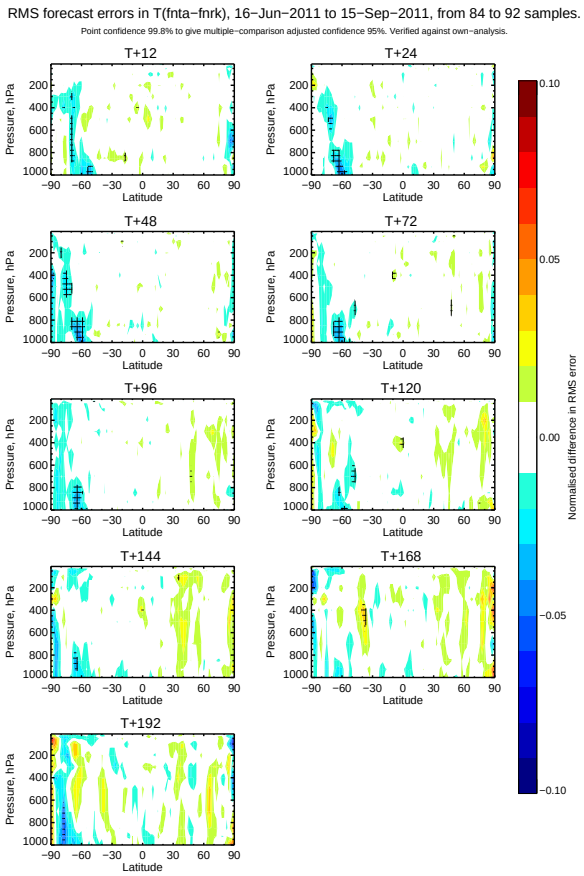

Figure 30: Normalised differences in the root mean squared forecast error between the experiment EXP1 (fnta) and the control experiment (fnrk) for the 0Z forecast of temperature at different pressure levels. Verification is against the experiment own-analysis.

however to reconsider relaxing the usage of MHS channel 5 measurements over sea as those observations in dry atmospheric conditions are considerably sensitive to the surface and not well modelled.

Results of assimilation experiments are encouraging towards a more extensive exploitation of MHS observations over sea and sea ice, though they show that the additional data are introducing biases which gradually corrupt slightly the first-guess in the Northern Hemisphere. Experiments have been run at a low resolution and will require some further testing at higher resolutions.

5 General conclusions

This study investigates an enhanced usage of satellite observations from the microwave sounders AMSU-A and MHS over land, high orography and sea ice. Here we briefly summarise the main findings of this work.

The active assimilation of the lowest-peaking of the MHS channels in the 183 GHz water vapour band over land has a systematic impact on the mean moisture analysis, which has been positively validated against independent GPS measurements from ground stations. As a result of these studies, MHS channel 5 is now actively assimilated over land in the latest ECMWF cycle (CY38R1).

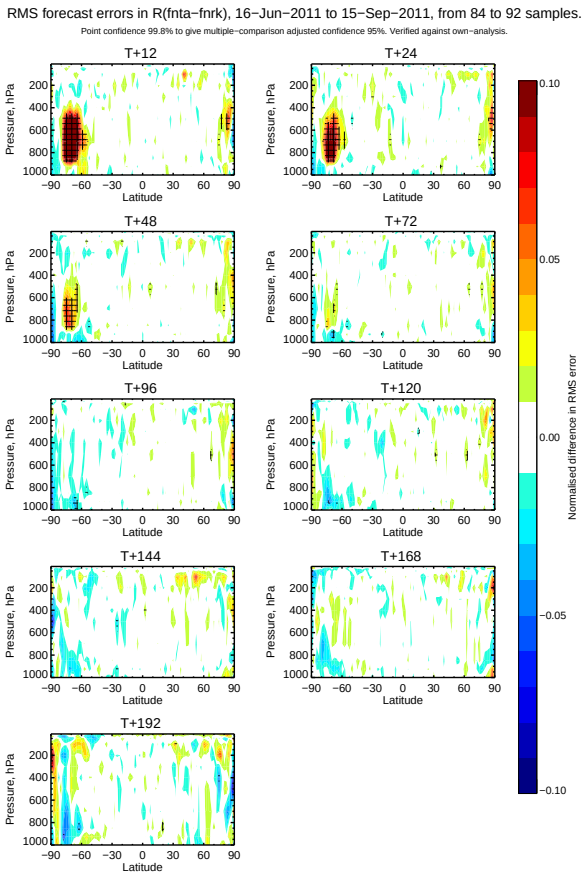

Figure 31: Normalised differences in the root mean squared forecast error between the experiment EXP1 (fnta) and the control experiment (fnrk) for the 0Z forecast of the relative humidity at different pressure levels. Verification is against the experiment own-analysis.

A new screening criterion has been tested to screen out radiance observations with too large a contribution from the surface. Is is based on single thresholds used globally per each relevant channel, and has allowed a more homogeneous coverage of the microwave sounding surface-sensitive channels. A considerable additional number of observations is assimilated in particular at outer scan positions (as those observations are less sensitive to the surface than the ones near nadir). However, results of assimilation experiments suggest that a unique global threshold per channel might not work well. In the rest of the fellowship we intend to pursue an alternative approach to the current screening of surface-sensitive microwave sounder observations with an observation error which would take into account different surface characteristics.

The assimilation of humidity sounding observations from MHS has been extended over sea ice and over sea at any skin temperature, with dynamically retrieved emissivities used over sea ice. Results of assimilation experiments are significantly positive for the forecast of the temperature, geopotential and winds in the Southern Hemisphere, though they show that the additional data are introducing small biases which gradually corrupt slightly the first-guess in the Northern Hemisphere. The results are however very encouraging towards a more extensive exploitation of MHS observations over sea and sea ice. We intend to follow this route in the rest of this EUMETSAT fellowship.

Acknowledgements

Enza Di Tomaso is funded by the EUMETSAT Fellowship Programme. Stephen English and Alan Geer are thanked for their help in this work. Anabel Bowen and Rob Hine are gratefully acknowledged for their help editing some of the figures.

References

Bock, O., M.N. Bouin, E. Doerflinger, P. Collard, F. Masson, R. Meynadier, S. Nahmani, M. Koit, K. Gaptia Lawan Balawan, F. Did, D. Ouedraogo, S. Pokperlaar, J.-B. Ngamini, J.P. Lafore , S. Janicot, F. Guichard, M. Nuret (2008), The West African Monsoon observed with ground-based GPS receivers during AMMA. J. Geophys. Res., 113, D21105.

Bormann, N., B. Krzeminski, P. Bauer (2009), Developments in the use of ATVOS data at ECMWF. Proceedings of the 2009 EUMETSAT Meteorological Satellite Conference, Bath, United Kingdom 21 - 25 September 2009, EUMETSAT P.55

Bouchard, A., F. Rabier, V. Guidard, F. Karbou (2010), Enhancements of Satellite Data Assimilation over Antarctica, Monthly Weather Review, 138(6), 2149-2173.

Cardinali, C. (2009), Monitoring the observation impact on the short-range forecast. Q. J. R. Meteorol. Soc. 135, 239-250.

Dee, D.P. (2004), Variational bias correction of radiance data in the ECMWF system. In Proceedings of the ECMWF Workshop on Assimilation of High Spectral Resolution Sounders in NWP. ECMWF, Reading, UK, 97-112.

Dow, J.M., R. E. Neilan, and C. Rizos (2009), The International GNSS Service in a changing landscape of Global Navigation Satellite Systems, J. Geodesy, 83, 191198.

English S. J., and T. J. Hewison (1998), A fast generic millimeter-wave emissivity model. Microwave Remote Sensing of the Atmosphere and Environment, T. Hayasaka et al., Eds., International Society for Optical Engineering (SPIE Proceedings), 3503, 288-300.

English, S. J. (2008), The Importance of Accurate Skin Temperature in Assimilating Radiances From Satellite Sounding Instruments. IEEE Transactions on Geoscience and Remote Sensing, 46(2), 403-408.

Geer, A. J., P. Bauer and P. Lopez (2009), Direct 4D-Var assimilation of all-sky radiances. Part II: Assessment, Q. J. R. Meteorol. Soc., 00, 1-27.

Harlow, R.C. (2011), Sea Ice Emissivities and Effective Temperatures at MHS Frequencies: An Analysis of Airborne Microwave Data Measured During Two Arctic Campaigns, IEEE Transactions on Geoscience and Remote Sensing, 49(4), 1223-1237.

Karbou, F., F. Rabier, J.-P. Lafore, J.-L. Redelsperger, O. Bock (2010), Global 4DVAR Assimilation and Forecast Experiments Using AMSU Observations over Land. Part II: Impacts of Assimilating Surface-Sensitive Channels on the African Monsoon during AMMA, Wea. Forecasting, 25, 2036.

Karbou, F., E. Grard, F. Rabier (2005), Microwave land emissivity and skin temperature for AMSU-A and -B assimilation over land. Q. J. R. Meteorol. Soc., 132, 2333-2355.

Kelly, G. and Bauer, P. (2000), The use of AMSU-A surface channels to obtain surface emissivity over land,

snow and ice for numerical weather prediction, In Proceedings of 11th International TOVS Study Conference, Budapest, Hungary, 167-179.

Krzeminski, B et al. (2008), EUMETSAT Fellowship first year report, ECMWF (available from the authors).

Liu, Q., F.Weng and S.J. English (2011), An Improved Fast Microwave Water Emissivity Model. IEEE Trans. Geosci. Remote Sens., 49, 1238-1250.

Ware, R.H. D. W. Fulker, S. A. Stein, D. N. Anderson, S. K. Avery, R. D. Clark, K. Droegemeier, J. P. Kuettner, and J. B. Minster (2000), Suominet: A real-time national GPS network for atmospheric research and education. Bulletin of the American Meteorological Society 81, 677-694.

6 Appendix

The active assimilation of MHS channel 5 has been tested for submission to the cycle upgrade (CY38R1) with some fixes to the estimation of emissivities for AMSU-A and MHS. These fixes are related to the update of what is called the emissivity 'atlas' (Krzeminski et al. 2008). The 'atlas' is a smoothed version of the dynamic emissivities updated with a Kalman Filter on a fixed grid, and it is used as backup and quality control for the dynamic emissivities. Here we show the changes in the 'atlas' in the experiment "channel 5 exp (2011)" described in Section 2 compared to the control.

In the control experiment the 'atlas' does not follow well sudden changes of the dynamic emissivities (for example in the case of melting snow). This is because the quality control on the dynamic emissivities used to update the 'atlas' emissivities is too tight, allowing only dynamic emissivities that differ by less than 0.06 from the 'atlas' values.

Figure 32 shows the timeseries for a given location in North Asia of 'atlas' emissivities and dynamic emissivities for 50 days of the experiments in the winter season. While in the control experiment, for this particular location, the atlas emissivities and dynamic emissivities diverge, the fixes applied in "channel 5 exp (2011)" let the 'atlas' be a smoothed version of the dynamic emissivities (as the 'atlas' was designed to be). Figure 33 shows the 'atlas' emissivity values for AMSU-A on MetOp-A in operations (bottom) and in the "channel 5 exp (2011)" (top) for a day in the summer period (for convenience only values greater than 0.7 are plotted). The unrealistic low emissivities over the Northern Hemisphere are corrected by the fixes applied in the 'atlas' update.

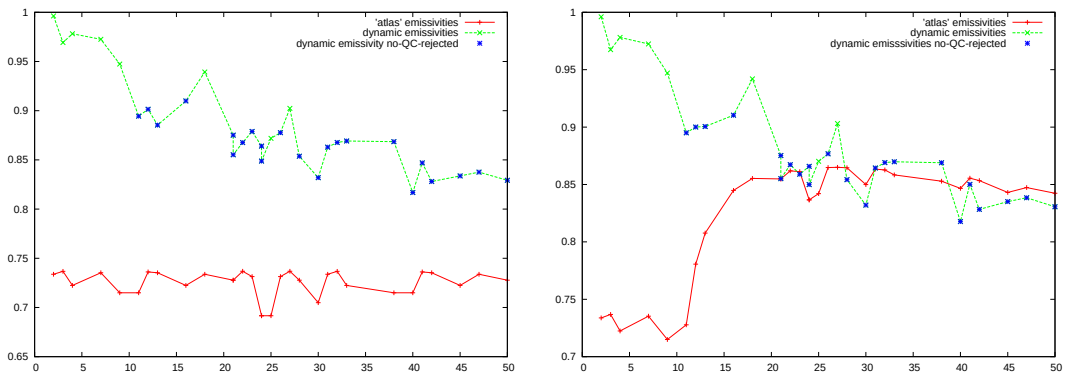

Figure 32: Timeseries of 'atlas' emissivities (red), dynamic emissivities (green), and dynamic emissivities not rejected by the quality control (blue) in the "ctl exp (2011)" experiment (left) and in the "channel 5 exp (2011)" experiment (right).

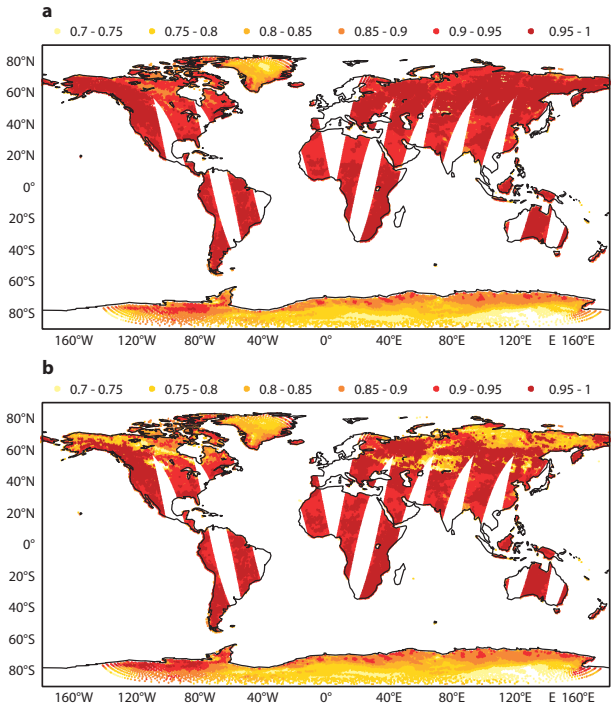

Figure 33: Atlas emissivities for ASMU-A on MetOp-A in the "channel 5 exp (2011)" experiment (top) and in operations (bottom) in a 12 hour time window in July 1 2011.